

Raman study of low-temperature-grown $\text{Al}_{0.29}\text{Ga}_{0.71}\text{As}/\text{GaAs}$ photorefractive materials

L. W. Guo* and Y. J. Han

Center for Condensed Matter Physics, Institute of Physics, Chinese Academy of Science, Beijing 100080, China

C. Y. Hu, P. H. Tan, and F. H. Yang

National Laboratory for Superlattices and Microstructures, Institute of Semiconductors, Chinese Academy of Science, Beijing 100083, China

Q. Huang and J. M. Zhou

Center for Condensed Matter Physics, Institute of Physics, Chinese Academy of Science, Beijing 100080, China

(Received 4 June 2001; published 13 March 2002)

We report on the observation of resonant Raman scattering in low-temperature-grown $\text{AlGaAs}/\text{GaAs}$ structure. Two kinds of excitation lights, 632.8 and 488 nm laser lines, were used to detect scattering signal from different regions based on different penetration depths. Under the *outgoing resonant* condition, up to fourth-order resonant Raman peaks were observed in the low-temperature-grown AlGaAs alloy, owing to a broad exciton luminescence in low-temperature-grown AlGaAs alloy induced by intrinsic defects and As cluster after post-annealing. These resonant peaks were assigned according to their fundamental modes. Among the resonant peaks, besides the overtones of the GaAs - or AlAs -like mode, there exist combination bands of these two kinds of modes. In addition, a weak scattering peak similar to the bulk GaAs longitudinal optical mode was observed in low-temperature Raman experiments. We consider the weak signal correlated with GaAs clusters appearing in AlGaAs alloys. The accumulation of GaAs in AlGaAs alloys was enhanced after annealing at high temperatures. A detailed study of the dependence of vibration modes on measuring temperature and post-annealing conditions is given also. In light of our experiments, it is suggested that a Raman scattering experiment is a sensitive microscopic probe of local disorder and, especially performed at low temperature, is a superior method in detecting and analyzing the weak interaction between phonons and electrons.

DOI: 10.1103/PhysRevB.65.125325

PACS number(s): 78.30.Fs, 61.72.Dd, 61.72.Ji, 63.20.Kr

I. INTRODUCTION

There is considerable current interest in low-temperature-(LT-) grown GaAs and related $\text{GaAs}/\text{AlGaAs}$ structures for the fabrication of isolating layer or ultrafast optical devices due to their high resistivity and ultrafast carriers recombination. The growth with an As-rich condition at LT allows incorporation of intrinsic defects including an As antisite, Ga vacancy, and their complex. The density and configuration of the intrinsic defects determine the conductivity of as-grown materials. Due to the hopping conductance among defective centers, the as-grown materials have low resistivity. However, after post-annealing, the excess As precipitated into As clusters that took as a defect center to capture carriers or depleted the carriers in the LT layer, so it rendered the LT layer with a high resistivity. Studying, controlling, and using these features have long been a main subject of material scientists. Up to now, a lot of research has been devoted to the LT-grown GaAs and related structures by electromagnetic and optical experiments.¹⁻⁸ However, to our best knowledge, there were few articles contributing to LT-grown AlGaAs ,^{9,10} and there was nearly no report on their characteristics studied by resonant Raman scattering. As is well known, Raman scattering has proved to be a useful technique for the observation of localized or quasilocated vibrational modes due to intrinsic defects in LT-grown GaAs . Additionally, AlGaAs , as a popularly used ternary alloy, was widely used in photorefractive devices and distributed Bragg reflectance (DBR) structure in vertical cavity surface emitting devices for indium-contained long-wavelength lasers. In the

former, LT- AlGaAs was used as a trap layer to hold enough charges. In the latter, the growth temperature for the AlGaAs is required to lower slightly in order to match the growth condition for InGaAs quantum wells and to avoid segregation of indium. Therefore, study of LT- AlGaAs is important to understand its structural and defect characteristics, interaction between electrons and phonons, and finding new features induced by (or related to) disorder or defects. In this paper, resonant Raman scattering was used to investigate the high-order Raman scattering features of LT- $\text{Al}_{0.29}\text{Ga}_{0.71}\text{As}$ and up to fourth-order resonant scattering peaks were observed clearly. Their origin and relation to the quality of LT- $\text{Al}_{0.29}\text{Ga}_{0.71}\text{As}$ alloy were discussed. Meanwhile, a comparative study of the dependence of the vibration modes in LT- AlGaAs on measurement temperature and post-annealing conditions is given also.

II. EXPERIMENTAL DETAILS

The sample was grown at 360 °C in a VG-V80H molecular beam epitaxy (MBE) system. A 1/4 two-inch semi-insulating GaAs (001) substrate was soldered on a Mo block with indium. The substrate temperature was measured by a thermocouple calibrated to the oxide film desorption temperature. The sample structure was designed for Stark geometry, and the photorefractive device consisted of 150 nm $\text{Al}_{0.29}\text{Ga}_{0.71}\text{As}$, GaAs (7.5 nm)/ $\text{Al}_{0.29}\text{Ga}_{0.71}\text{As}$ (4 nm) multiple quantum wells (MQW's) followed by another 150 nm $\text{Al}_{0.29}\text{Ga}_{0.71}\text{As}$ capped with a 2-nm GaAs protective layer. During growth, the pressure was kept at 3.4×10^{-7} Torr. Af-

ter growth, the sample was cut into several pieces and each piece was subjected to isochronal 30 s rapid thermal annealing (RTA) at temperatures ranging from 500 to 900 °C with a step of 100 °C under a protection of argon gas ambient. To prevent As loss from the surface, each piece of samples was covered with a piece of GaAs substrate during annealing.

After the RTA treatment, a Raman scattering experiment was performed at low and room temperatures for as-grown and post-annealed samples. Unpolarized Raman scattering spectra were recorded in the backscattering geometry on the (001) face of the samples. Low-temperature measurements were carried out in a variable temperature stainless-steel cryostat where low temperature was generated by a closed He cycle and temperature can be adjusted from 10 to 300 K. A 632.8-nm line of He-Ne laser and a 488-nm line of Ar⁺ laser were used as excitation sources. The scattering light was detected by a charge coupled device (CCD) detector.

III. RESULTS AND DISCUSSION

This section will be divided into two subsections. In Sec. III A, we will discuss the resonant Raman scattering data excited by the 632.8-nm laser line; in Sec. III B, the nonresonant Raman scattering spectra, excited by the 488-nm line, are analyzed. In each section, Raman scattering experiments performed at low temperature and room temperature are discussed separately.

It is known that both energies of excitation lights used here are larger than the band gap energy of Al_{0.29}Ga_{0.71}As alloy. The penetration depths are about 390 and 110 nm for a 632.8- and a 488-nm excitation lights at normal incidence into Al_{0.29}Ga_{0.71}As alloy,¹¹ respectively. When a 632.8-nm line was used in our experiments, detected Raman scattering signals came not only from the upper Al_{0.29}Ga_{0.71}As trap layer, but also from the lower GaAs/Al_{0.29}Ga_{0.71}As MQW region. And when a 488-nm line was used, a signal from the upper Al_{0.29}Ga_{0.71}As trap layer was observed only, because the penetration depth 110 nm is shorter than the thickness 150 nm of the upper Al_{0.29}Ga_{0.71}As trap layer. So using different excitation lights made vibrational features from different structural regions to be distinguished clearly.

A. Resonant Raman scattering excited by a 632.8-nm laser

1. Raman spectra measured at room temperature

First of all, a Raman spectrum from a sample annealed at 800 °C was measured at room temperature with a 632.8-nm excitation line, as shown in Fig. 1. Since the photon energy of a 632.8-nm line is slightly larger than that of the absorption band of Al_{0.29}Ga_{0.71}As alloy, an *outgoing resonant* condition is satisfied (i.e., the energy of the scattered light equals an electronic transition energy). Therefore, the high-order resonant Raman scattering from phonons was enhanced and observed in the spectrum of Fig. 1, except the first-order Raman peaks. In the case of AlGaAs alloy, the long-wavelength optical phonons around the Brillouin-zone center display a two-mode behavior throughout the whole composition range.¹² There are pairs of longitudinal (LO) and transverse (TO) optical modes called GaAs like and AlAs like.

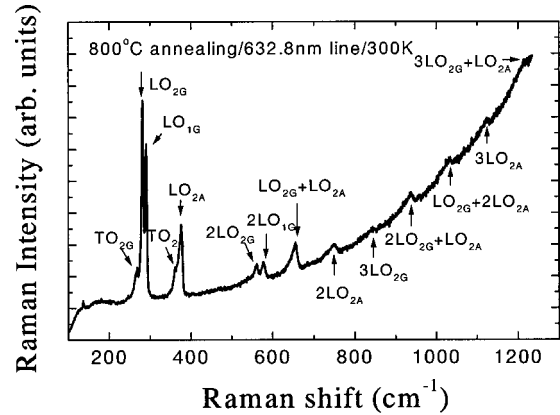


FIG. 1. Resonant Raman scattering spectra for the 800 °C-annealed sample measured at room temperature using a 632.8-nm excitation light. The arrows show the positions of the Raman peaks.

Therefore, two sets of strong peaks observed in Fig. 1 are related to their first-order Raman scattering peaks, located in low frequency with wave numbers less than 400 cm⁻¹. Comparing with the well-known GaAs- and AlAs-like vibrational modes, the peaks at 376.2, 290, and 281.5 cm⁻¹ are assigned to LO vibrational modes of the Al-As bond in the Al_{0.29}Ga_{0.71}As layer and Ga-As bond in GaAs QW's and Al_{0.29}Ga_{0.71}As layer, respectively. They were expressed as LO_{2A}, LO_{1G}, and LO_{2G}, correspondingly. The subscripts G and A and 1 and 2 represent the vibrational modes of Ga-As (G) and Al-As (A) bonds and the vibrational mode coming from the GaAs QW (1) and the Al_{0.29}Ga_{0.71}As trap layer (2) or the Al_{0.29}Ga_{0.71}As barriers (2), respectively. The LO_{2A} peak is in good agreement with the Kim and Spitzer's result for Al_{0.29}Ga_{0.71}As alloy,¹³ but the LO_{2G} peak is 3 cm⁻¹ higher than their value 278.5 cm⁻¹ with 1% deviation. We attributed the deviation to effect of post-annealing, which is also observed in spectra of samples annealed at different temperatures discussed later. Obviously, a weak peak located at 267 and 360.9 cm⁻¹ related to the TO phonons of GaAs- and AlAs-like in Al_{0.29}Ga_{0.71}As alloy denoted as TO_{2G} and TO_{2A}, which is in good agreement with TO modes in bulk Al_{0.29}Ga_{0.71}As alloy.¹³ According to the polarization selection rule for the first-order Raman scattering in zinc-blende-type crystals, the LO mode from the (001) surface is allowed and the TO mode is forbidden in the backscattering geometry. The appearance of the TO phonon peak here is ascribed to local disorder due to incorporated defects or precipitation of excess As in post-annealed LT sample. In addition, several high-order Raman peaks now rode over the luminescence of upper Al_{0.29}Ga_{0.71}As trap layer, fulfilling the condition of outgoing resonance. It is seen that up to fourth-order resonant Raman bands appeared, which is seldom observed in AlGaAs ternary alloy. The origin of observing these resonant peaks was there existed a broad luminescence band in the LT-grown Al_{0.29}Ga_{0.71}As alloy, which made the *outgoing resonant* condition (phonon replica) satisfied easily. The broad luminescence originated from the degradation of material quality by intrinsic defects or As clusters in annealed samples. Usually, these high-order scattering bands are due to successive first-order Raman scattering. They are the over-

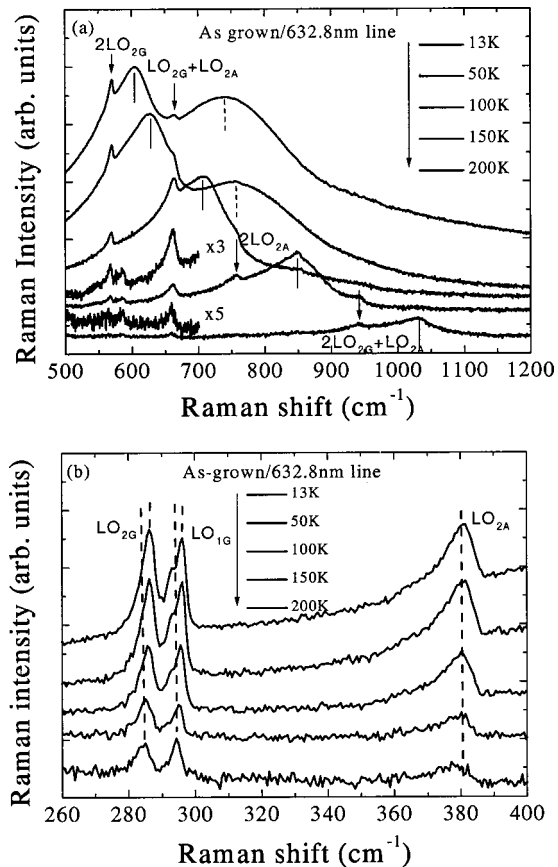


FIG. 2. Raman spectra for the as-grown sample measured at 13–200 K using a 632.8-nm excitation light, (a) for the high-order resonant Raman scattering, where the arrows, solid lines, and dashed lines mark the peaks of phonon modes, exciton, and defect luminescence, respectively. (b) For the first-order Raman scattering, the dashed lines is a guide to the eye to see the peak shift with temperature.

tones of the same fundamental modes or combination bands of different fundamental modes. So the vibrational energies of these modes are the sum of the corresponding first-order modes. They are assigned to $2LO_{2G}$ (561.9 cm^{-1}), $2LO_{1G}$ (579.1 cm^{-1}), $LO_{2G}+LO_{2A}$ (655.3 cm^{-1}), $2LO_{2A}$ (750.7 cm^{-1}), $3LO_{2G}$ (844 cm^{-1}), $2LO_{2G}+LO_{2A}$ (938 cm^{-1}), $LO_{2G}+2LO_{2A}$ (1032 cm^{-1}), $3LO_{2A}$ (1129 cm^{-1}), and $3LO_{2G}+LO_{2A}$ (1220.1 cm^{-1}), according to their fundamental modes with error less than 2 cm^{-1} . It is noted that except the $2LO_{1G}$ peak, all of the high-order peaks are from $Al_{0.29}Ga_{0.71}As$ alloy, owing to the resonant enhancement to phonon scattering in $Al_{0.29}Ga_{0.71}As$ layer. Among the high-order resonant peaks, it is seen that besides the overtones of the GaAs- or AlAs-like mode, there existed the combination bands of the two kinds of modes.

2. Raman spectra measured at low temperature

Besides the measurement of Raman scattering at room temperature, a low-temperature Raman scattering is conducted in the as-grown sample. Figure 2 shows the Raman spectra measured at 13–200 K using a 632.8-nm excitation light, where the high- and first-order modes are shown sepa-

rately in Figs. 2(a) and 2(b). It is known that varying the measurement temperature means a change of lattice temperature, also a change of its band gap. Therefore, the resonant scattering condition was varied, leading to different resonant peaks to be observed. In Figs. 2(a) and 2(b), the curves were plotted in half-logarithm coordinates and were shifted vertically to see clearly. In Fig. 2(a), the solid and dashed lines point to the peaks of exciton and defect luminescence, respectively, and the arrows mark the corresponding resonant Raman scattering peaks. As the temperature is lower than 100 K, only the second-order Raman peaks were observed. With increasing temperature, the third-order Raman peak was seen. It is confirmed that the high-order phonon scattering could be activated while the energy difference of incident and scattering light is equal or near the sum of phonon vibrational energies. With further increasing the temperature to 200 K, the exciton luminescence became weak and there is no resonant Raman peak appearing in the high-energy side of the exciton peak, compared with the one that appeared in the low-energy side of the exciton peak. It is noted that besides the high-order modes from the $Al_{0.29}Ga_{0.71}As$ alloy, a weak second-order resonant mode from the GaAs QW was observed at a temperature higher than 150 K. In Fig. 2(a), the magnified spectra of the peak are shown above their corresponding curves, where the high-energy one in the couple of peaks was from the GaAs QW's owing to an increase of the phonon state density with temperature. In addition, a broad luminescence peak marked with a dashed line appeared in 13 and 50 K spectra with energy 16.8 meV lower than its exciton peak. We attributed the peak to luminescence from shallow defects, because its binding energy is small and the peak shifted with the exciton peak as the temperature varied. It is found the luminescence quenched at a temperature above 70 K.

In Fig. 2(b), the evolution of the first-order Raman peaks versus temperature is shown. It is found that there are no TO modes in Fig. 2(b) compared with that observed in Fig. 1. We consider more lattice disorder was induced by As clusters in post-annealed samples, although there exists intrinsic defects in the as-grown sample. The atomic arrangements near or beside the As cluster inevitably deviated from its ideal structure, leading to the activation of TO modes in the annealed sample. In spectra of 13–100 K, a shoulder faintly appeared on the low-energy side of the GaAs LO_{1G} peak and the shoulder became undiscernible at a temperature above 100 K. The wave number difference between the shoulder and its main peak is about 3 cm^{-1} . With increasing temperature, the shoulder merged into its main peak owing to the effect of thermal broadening on the vibration mode. Reasonably, we consider that there are two possible reasons related to the shoulder. One was strain induced by excess As incorporated in the as-grown LT-GaAs QW's. The nonuniform strain might cause a local distortion of Ga-As bonds, which was too weak to be detected at room temperature. The other possible reason is there exists microscopic GaAs clusters in the $Al_{0.29}Ga_{0.71}As$ alloy, which inference was confirmed in the annealed samples and will be discussed later in part of Fig. 3. Our experiment here suggests that Raman scattering especially performed at low temperature is a superior method

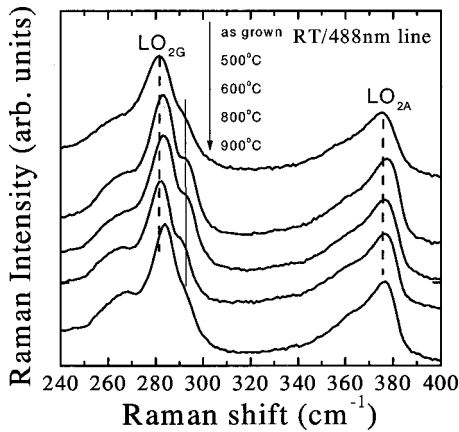


FIG. 3. Raman spectra for as-grown and post-annealed samples measured at room temperature using a 488-nm excitation light. The curves from up to down correspond to as-grown to 900 °C-annealed samples. The dashed lines are guides to the eye to show the shift of the peaks with annealing temperature.

in observing and distinguishing weak scattering and local disorder in crystal.

Observing Fig. 2(b) carefully, it is seen that three sets of peaks showed a similar shift to low frequency with increasing temperature, as a consequence of thermal expansion. However, the AlAs-like peak shifted little and showed a prominent asymmetric broadening towards low frequency. The reason is there is a high anharmonicity of AlAs-like modes as compared with GaAs-like modes, which can be associated in a first approximation with the smaller reduced mass of AlAs compared with GaAs.^{14,15} The shift of the high-order vibrational modes with temperature, as shown in Fig. 2(a), was consistent with the sum of their corresponding first-order mode shift as observed in Fig. 2(b).

B. Nonresonant Raman scattering excited by a 488-nm laser

1. Raman spectra measured at room temperature

A study of the annealing effect on the phonon characteristic of LT-AlGaAs alloy is necessary to understand the evolution of intrinsic defects and roles of As clusters. Figure 3 shows the Raman spectra of the as-grown and post-annealed samples in a half-logarithmic coordinate, excited with a 488-nm line and performed at room temperature. The spectra had been shifted vertically for comparison. As mentioned above, while a 488-nm excitation light was used, only phonons in the $\text{Al}_{0.29}\text{Ga}_{0.71}\text{As}$ trap layer took part in Raman scattering, so crystalline features of the $\text{Al}_{0.29}\text{Ga}_{0.71}\text{As}$ trap layer were detected. Since it was far away from the resonant scattering conditions while a 488-nm line was used as an excitation light, the first-order Raman scattering was observed. It is seen in Fig. 3 that the linewidth of the GaAs-like LO_{2G} peaks was narrowed with increasing annealing temperature and the peaks showed a slight shift of about 1 cm^{-1} to high energy after post-annealing for 30 s at a temperature above 500 °C. Both of the features are similar to the results observed in post-annealed LT-GaAs samples.¹⁶ We ascribed the effects to the improvement of crystal quality and the

relaxation of tensile strain induced by the incorporation of excess As after post-annealing at high temperature. Comparing the peaks, the AlAs-like LO_{2A} peaks were not only broader than those of GaAs-like LO_{2G} peaks, but also their asymmetry is prominent as observed in Fig. 2(b). The broader linewidth and asymmetry can be ascribed to a finite phonon correlation length and the higher anharmonicity of AlAs-like modes as discussed in Fig. 2(b). The defects and disorder in the annealed sample enhanced the anharmonicity of phonon.¹⁷ However, no matter what was the annealing temperature, the position of AlAs-like LO_{2A} peak maintained nearly no change. According to the measured AlAs-like phonon energy, the composition x of the AlGaAs alloy can be deduced from the interpolation expression $\omega_{\text{LO}_{2A}} = 359.7 + 70.8x - 26.8x^2 \text{ (cm}^{-1}\text{)}$.¹⁸ The calculated value of x equals 0.27. This value is close to the composition 0.29 estimated from an oscillation period of a reflection of high-energy electronic diffraction (RHEED) for calibration of the growth rates of GaAs and AlGaAs alloys.

It is noted that there were two sets of shoulders on both sides of the GaAs-like LO_{2G} peak. One is located at the low-energy side around 268 cm^{-1} related to the GaAs-like TO_{2G} peak, whose scattering intensity is enhanced with increasing annealing temperature. The phenomenon suggests that annealing enhanced local disorder in the structure and destroyed the forbidden rule to the TO mode in backscattering geometry. Another shoulder located at the high-energy side around 292 cm^{-1} is in the same frequency as pure GaAs mode LO_{1G} from the GaAs QW's described in Fig. 1. As mentioned above, the observed scattering signal in Fig. 3 should be from the upper $\text{Al}_{0.29}\text{Ga}_{0.71}\text{As}$ layer only, while a 488-nm line was used. It is seen that the shoulder had a close relationship with the annealing temperature. It is hardly discernible in as-grown and 900 °C-annealed samples, but became prominent in the samples annealed at 500, 600, and 800 °C. Consequently, it is inferred that the shoulder positioned at 292 cm^{-1} cannot be from the GaAs QW's. We suggested that the shoulder came from the phonon scattering in the microscopic GaAs clusters presented in the upper $\text{Al}_{0.29}\text{Ga}_{0.71}\text{As}$ layer, which effect was enhanced after annealing as-grown samples at 500, 600, and 800 °C. Before our results, the presence of GaAs clusters in AlGaAs alloys was reported with high Al composition only, but not in the low one as $x=0.3$ grown in normal conditions.¹⁹ We consider the intrinsic defects incorporated into the LT-AlGaAs assisted accumulation of GaAs in AlGaAs alloy during annealing.

2. Raman spectra measured at low temperature

To confirm the inference of appearing GaAs clusters in LT-AlGaAs further, the Raman scattering spectra excited by a 488-nm laser were performed at LT. The spectra of as-grown and 800 °C-annealed samples are shown in Figs. 4(a) and 4(b), respectively, in a half-logarithmic coordinate, where the curves were shifted vertically to compare clearly. It is seen that there are two main peaks appearing in each curve: one is a GaAs-like mode and another is an AlAs-like mode similar to the ones observed in Fig. 3. Observing Fig. 4, it is found that there is a weak peak (marked with a solid line) appearing in the high-energy side of the GaAs-like

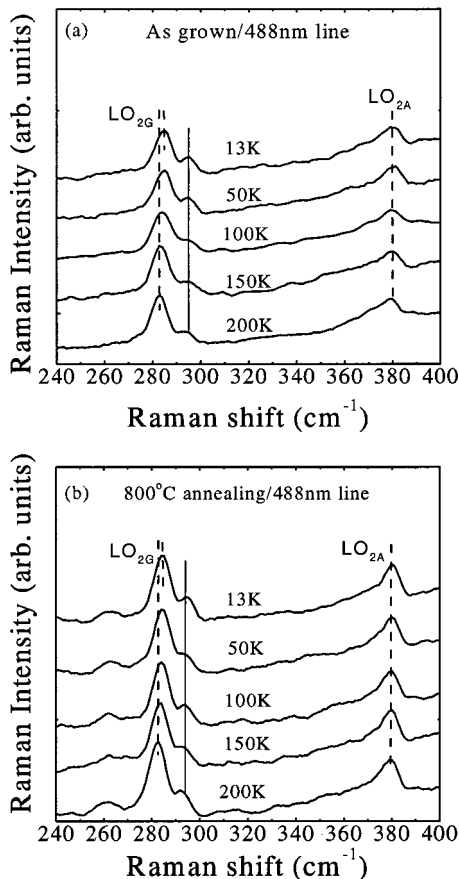


FIG. 4. Raman spectra for the as-grown and 800 °C-annealed samples measured at 13–200 K using a 488-nm excitation light, (a) for as-grown sample and (b) for 800 °C-annealed samples. The dashed and solid lines are guides to the eye to show the shift of the peaks with measurement temperature.

peak. According to the analysis of Fig. 3, it is known that the weak peak is related to the GaAs cluster formed in the LT-AlGaAs layer. Owing to the suppression of the thermal expansion effect on the GaAs-like mode (LO_{2G}) in the LT-AlGaAs layer while measured at LT, the scattering peak from the GaAs clusters becomes clear even in the as-grown sample. It is seen that the Raman scattering signals are stronger in the 800 °C-annealed sample than in the as-grown sample at the same LT measurement. So it can be well understood why the weak peak is easier to discern in the 800 °C-annealed sample than in the as-grown sample while measured at room temperature as shown in Fig. 3. It suggests that high-temperature annealing enhanced the GaAs accumulated in GaAs clusters in LT-AlGaAs layers. Owing to the weak peak overlapping with the GaAs-like LO_{2G} , the cluster size cannot be precisely deduced at a moment based on its linewidth. Further study is needed and necessary for under-

standing the process of GaAs accumulation in LT-AlGaAs alloys. Besides the weak peak, there is a shoulder appearing in the low-energy side of the LO_{2G} peak in the 800 °C-annealed sample, but not in the as-grown sample. The shoulder originates from the TO_{2G} mode, which is similar to the one observed in Fig. 1. There is no TO mode in Fig. 4(a) for the as-grown sample consistent with the result of Fig. 2(b) while measured using a 632.8-nm laser line. From our results in Fig. 4, it is further proved that the Raman scattering experiment performed at LT is a sensitive probe of weak local ordering and disordering.

IV. CONCLUSIONS

In summary, a Raman scattering experiment was used to study the crystalline characteristics and defective features in as-grown and post-annealed AlGaAs/GaAs photorefractive material grown at LT by solid-source MBE. Due to the special features of the LT sample, up to fourth-order Raman scattering peaks were observed in the $Al_{0.29}Ga_{0.71}As$ alloy, which is seldom observed in AlGaAs alloys fabricated in normal growth conditions. All of the high-order resonant peaks were assigned according to their fundamental modes. Besides the overtones of the GaAs- or AlAs-like mode, there exists the combination bands of the two kinds of modes, too. This result shows that a material with broad exciton luminescence is favorable to observe the high-order resonant Raman scattering bands. As measured at LT, a weak scattering peak similar to the bulk GaAs LO mode was observed owing to the suppression of the thermal broadening effect. We consider that the weak peak is correlated with the GaAs cluster appearing in $Al_{0.29}Ga_{0.71}As$ alloy. Annealing at 500, 600, and 800 °C enhanced the accumulation of GaAs in LT-AlGaAs alloy. These results reveal that there exists more or less microscopic GaAs clusters in our as-grown LT-AlGaAs layer besides the well-known As antisite, Ga vacancy, and As cluster. All of these results proved that the Raman scattering experiment, especially performed at low temperature, is a superior method in detecting and analyzing the weak interaction between phonons and electrons. A deep study of LT-AlGaAs ternary alloy by Raman scattering will reveal phenomena that may be difficult to find by other experimental techniques.

ACKNOWLEDGMENTS

Some of the authors thank the support of the Natural Sciences Foundation of China under Contract No. 69896260. One of the authors (L.W.G.) would like to give her thanks to the National Laboratory for Superlattices and Microstructures, Institute of Semiconductors, Chinese Academy of Science, for providing experimental measurements of Raman scattering.

*Corresponding author. Electronic address:

lwguo@aphy.iphy.ac.cn

¹M. R. Melloch, J. M. Woodall, and E. S. Harmon, *Annu. Rev. Mater. Sci.* **25**, 547 (1995).

²D. C. Look, *Thin Solid Films* **231**, 61 (1992).

³D. C. Look, D. C. Walters, M. Mier, C. E. Stutz, and S. K. Brierley, *Appl. Phys. Lett.* **60**, 2900 (1992).

⁴M. Missous, *Mater. Sci. Eng., B* **44**, 304 (1997).

⁵X. Liu, A. Prasad, J. Nishio, E. R. Weber, Z. Liliental-Weber, and W. Walukiewicz, *Appl. Phys. Lett.* **67**, 279 (1995).

- ⁶G. Segschneider, T. Dekorsy, H. Kurz, R. Hey, and K. Ploog, *Appl. Phys. Lett.* **71**, 2779 (1997).
- ⁷P. W. Yu, D. C. Reynolds, and C. E. Stutz, *Appl. Phys. Lett.* **61**, 1432 (1992).
- ⁸D. D. Nolte, *J. Appl. Phys.* **85**, 6259 (1999).
- ⁹D. D. Nolte, M. R. Melloch, J. M. Woodall, and S. E. Ralph, *Appl. Phys. Lett.* **62**, 1356 (1993).
- ¹⁰S. Fleischer, C. D. Beling, S. Fung, W. R. Nieveen, J. E. Squire, and J. Q. Zheng, *J. Appl. Phys.* **81**, 190 (1997).
- ¹¹L. Pavesi and M. Guzzi, *J. Appl. Phys.* **75**, 4779 (1994).
- ¹²A. S. Barker, Jr. and A. J. Sievers, *Rev. Mod. Phys.* **47**, S1 (1975).
- ¹³O. K. Kim and W. G. Spitzer, *J. Appl. Phys.* **50**, 4362 (1979).
- ¹⁴J. Jimenez, E. Martin, A. Torres, and J. P. Landesman, *Phys. Rev. B* **58**, 10 463 (1998).
- ¹⁵D. Vanderbilt, S. G. Louie, and M. L. Cohen, *Phys. Rev. B* **33**, 8740 (1986).
- ¹⁶M. Tani, K. Sakai, H. Abe, S. Nakashima, H. Harima, M. Hangyo, Y. Tokuda, K. Kanamoto, Y. Abe, and N. Tsukada, *Jpn. J. Appl. Phys., Part 1* **33**, 4807 (1994).
- ¹⁷P. Verma, S. C. Abbi, and K. P. Jain, *Phys. Rev. B* **51**, 16 660 (1995).
- ¹⁸S. Adachi, *J. Appl. Phys.* **58**, R1 (1985).
- ¹⁹P. Lao, W. C. Tang, A. Madhukar, and P. Chen, *J. Appl. Phys.* **65**, 1676 (1989).